The Effect of Intentionally Perforating the Floor of the Pulp Chamber on Pulpal Healing after Tooth Replantation in Mice

Hiroto SANO

Division of Clinical Chemistry,

Niigata University Graduate School of Health Sciences,

Niigata, Japan

髄床底部への意図的穿孔形成がマウス歯の再植後の歯髄治癒過程に及ぼす影響

佐野拓人

新潟大学　大学院保健学研究科 検査技術科学分野

臨床化学研究室

ABSTRACT

Objectives: Shortening the root of a mouse molar prior to tooth replantation results in early revascularization in the pulp cavity and activation of the dental pulp quiescent stem cells. This study aimed to elucidate the effects of perforating the floor of the pulp chamber on pulpal healing after tooth replantation in order to determine whether this strategy is a valid methodology to promote early revascularization into the pulp.

Methods: The maxillary first molars of three-week-old Crlj:CD1 mice were extracted and repositioned into the original socket: the left teeth were immediately replanted (control group: CG), whereas the floor of the pulp chamber of the right teeth was perforated with a tungsten carbide bur before tooth replantation (experimental group: EG). The samples were collected from three days to eight weeks after the operation. In addition to the TUNEL assay, immunohistochemistry for Nestin, CK14, and Ki-67 was conducted.

Results: Early revascularization occurred with the decrease of apoptosis and an increase in cell proliferation to facilitate the pulpal healing in the EG compared with the CG. The rate of Nestin-positive perimeter in the distal root significantly increased on days 5 and 14 as well as Nestin-positive hard tissue on day 14. On day 7, the number of epithelial cell rests of Malassez in the EG significantly decreased, making the EG susceptible to

ankylosis at the floor.

Conclusions: Intentionally perforating the floor of the pulp chamber provides a route *via* the floor for early revascularization, resulting in the better pulpal healing after tooth replantation.

Key words: Blood supply; Dental pulp; Dentinogenesis; Mice; Tooth replantation

1. Introduction

Incomplete or complete dislocation of teeth frequently occurs following trauma. Permanent teeth suffer from avulsion at an approximate rate of 0.5%−3% among trauma cases in clinical dentistry, and tooth replantation is the first choice for treatment [1]. The complications associated with tooth replantation include pulp necrosis and obliteration, arrested or incomplete root formation, replacement resorption, internal root resorption, loss of attached gingiva, and tooth loss [2-4]. Pulpal healing patterns have a significant impact on the prognosis of replanted teeth [5, 6]. Inducing early dentin formation in the pulp cavity is essential for the optimal healing process of roots or periodontal tissue after tooth replantation, since the replanted teeth, in which the pulp cavity is replaced with bone, easily suffer root resorption and ankylosis [7]. The root development of replanted teeth, or the size of apical foramina, has a greater impact on pulpal healing [8-10]. Pulpal healing of the replanted tooth is expected if the roots are immature, whereas pulpectomy after or during operation is generally inevitable in the case of replanted teeth with matured roots that fail to establish revascularization [9, 10]. Previous animal investigations have shown that transplanting teeth with incomplete roots enhances pulpal healing [11], as well as expanding the apical foramina by apicoectomy of permanent teeth prior to replantation [12]. Transient root apical resorption may occur in

the pulpal healing process after tooth replantation of avulsed mature teeth [13]. Thus, the maintenance of a sufficient route for revascularization is an essential factor for pulpal healing.

The source of cells engaged in pulpal repair after tooth injuries is the dental pulp stem and progenitor cells. Previous research has identified two types of stem cells: active and quiescent stem cells [14]. The prenatal labeling method has been established to label dental pulp quiescent stem cells with prenatal administration of 5-bromo-2-deoxyuridine in the wild-type mice or doxycycline in TetOP–histone 2B (H2B)–green fluorescent protein (GFP) mice, using their characteristics of asymmetric cell division [15-19]. A combination of *in vivo* and *in vitro* animal models for tooth injury and a pulse-chase paradigm with prenatal labeling techniques have shown that label-retaining cells [LRCs] (putative quiescent stem and progenitor cells) localize to the subodontoblastic layer (SOBL) and the perivascular niche of central pulp tissue and differentiate into odontoblast-like cells (OBLCs) after exogenous stimuli [6, 17, 19-24].

At least two types of pulpal healing patterns occur after tooth replantation: dentin and bone tissue formation. Maintaining quiescent stem and progenitor cells is probably a critical factor in inducing OBLC differentiation [20]. Intentional resection of the root before tooth replantation is effective in revascularization in the pulp cavity and

promotion of pulpal healing, suggesting that normoxia apart from hypoxia in the pulp cavity after tooth replantation is a prerequisite for activation of dental pulp quiescent stem cells [25]. However, stem cells from apical papilla (SCAP) [26] are present in the apical papilla, and resecting the root leads to the loss of SCAP, despite early revascularization. SCAP have the ability to differentiate into OBLCs [26] and have a significantly higher proliferative activity and mineralization capability after differentiation than dental pulp stem cells (DPSCs) [27]. Thus, losing SCAP as cell resources associated with pulpal healing may have a negative impact on the long-term prognosis of the replanted teeth. This study aimed to examine the hypothesis that intentionally perforating the floor of the pulp chamber before tooth replantation promotes early revascularization of the pulp cavity of the replanted tooth and consequently contributes to accelerate pulpal healing. Nestin and Ki-67 antibodies were used to identify the odontoblast/OBLC differentiation and proliferating cells, respectively. Because the epithelial cell rests of Malassez (ERM) have been suggested to be involved in the maintenance of the periodontal space [28], CK14 antibody was used to evaluate the extent of damage to the ERM caused by perforation at the floor of the pulp chamber. This new method could be expected to preserve the root length and presence of the SCAPs and contribute to improving the pulpal healing of injured teeth.

2. Materials and methods

2.1. Animals

Male Crlj:CD1 (ICR) mice (three weeks old) (Charles River Laboratories Japan, Yokohama, Japan) were used. The animals were maintained in a specific pathogen-free, temperature-controlled environment with free access to food and water. All animal experiments were conducted in compliance with ARRIVE guidelines and a protocol that was reviewed by the Institutional Animal Care and Use Committee and approved by the President of Niigata University (Approval number: SA00784).

2.2. Tooth replantation

Under deep anesthesia with a mixed solution (0.05–0.1 mL/10 g) of Domitor® (1.875 mL: Nippon Zenyaku Kogyo Co, Ltd, Koriyama, Japan), midazolam (2 mL: Sandoz KK, Tokyo, Japan), Vetorphale® (2.5 mL: Meiji Seika Pharma Co, Ltd, Tokyo, Japan), and physiological saline (18.625 mL), both the right and left maxillary first molars (M1) of ICR mice were extracted (Nakakura-Ohshima et al., 2021). The left teeth were immediately replanted (control group: CG), whereas the floor of the pulp chamber of the right teeth was perforated with a tungsten carbide bur (diameter = 0.5 mm) before tooth replantation (experimental group: EG). The size of the perforation area was

measured in the sections of the EG at days three and five after operation using Image J software (Image J 1.53k, National Institutes of Health [NIH], Bethesda, MD). The average diameter of the perforation was 178 ± 98 μm.

2.3. Tissue preparation

Materials were collected from 31 animals (Fig. 1). The detailed procedure was described in the previous study [29]. The animals were perfused with 4% paraformaldehyde in a 0.1 M phosphate buffer (pH 7.4) under deep anesthesia. Following decalcification in a 10% EDTA-2Na solution, the specimens were dehydrated, embedded in paraffin, and cut sagittally into 4 μm sections. The sections were processed for hematoxylin and eosin staining and immunohistochemistry.

2.4. Immunohistochemical analysis

Immunohistochemistry for Nestin and Ki-67 was described elsewhere [29]. For CK14, anti- CK14(mouse monoclonal, #ab7800, Abcam plc, Cambridge, UK;1:50 dilution) was used. Apoptosis was quantified by terminal deoxynucleotidyl transferase-mediated dUTP nick end labeling (TUNEL) with the ApopTag Peroxidase In Situ Apoptosis Detection Kit (Merk Millipore, Billerica, MA, USA).

2.5. Micro-focus computed tomography (μCT) imaging

The μCT imaging was performed for samples on week four and eight using the ScanXmate-D100SS270 (Comscantecno Co. Ltd., Yokohama, Japan). The μCT settings were as follows: slice thickness, 12.68 μm; magnification, ×20.04; voltage, 80 kV; and electrical current, 58 μA. The maxillae were reconstructed using a software program (TRI/3D Bon, Ratoc System Engineering, Tokyo, Japan) to evaluate the three-dimensionally reconstructed views of the maxillae including the M1.

2.6. Statistical analysis

The rate of Nestin-positive perimeter on the pulp-dentin border in the mesial and distal pulps was measured in sections immunohistochemically stained for Nestin using the WinROOF image processing software (Mitani Corp., Tokyo, Japan) and Image J software (Image J 1.53k, NIH). The rate of hard tissue formation was measured in sections immunohistochemically stained for Nestin using the WinROOF image processing software (Mitani Corp.) and Image J software (Image J 1.53k, NIH). The number of ERM was calculated in sections immunohistochemically stained for CK14 using Image J software (Image J 1.53k, NIH), excluding areas with ankylosis. Apoptosis was quantified, and the rate of Ki-67- and TUNEL-positive cells was calculated

according to the previous study [25]. A picture was taken using the same grid and magnification (2.1×10^4 μm^2). The rate of Ki-67-positive cells in the picture was calculated using a computerized image analysis system, Patholoscope ver.1.2.1 (Mitani Corp.). In the case of the root area, two pictures were taken for each of the mesial and distal root pulp in the sagittal section of each sample. The rate of Nestin-positive perimeter and Ki-67/TUNEL-positive cells and the number of ERM/$3.0x10^5$ μm^2 of periodontal ligament among different stages after tooth replantation was compared using one-way analysis of variance followed by the Bonferroni test for multiple comparisons and the rates and number between different groups were compared using two-tailed Student's *t*-test with statistical software after the confirmation of data normality and homogeneity of variance (SPSS 16.0J for Windows; SPSS Japan, Tokyo, Japan). The samples showing no normal distribution were compared by Kruskal Wallis test followed by the Bonferroni test for multiple comparisons for more than three groups or Mann Whitney U test for two groups.

Results

3.1 Chronological changes in the Nestin expression in the replanted teeth

In the untreated tooth, differentiated odontoblasts showed Nestin-positive reactions

throughout the dental pulp (Fig. 2). Three days after tooth replantation, Nestin expression was observed in the survived odontoblasts or newly differentiated OBLCs beneath the root pulp of the CG and EG, although the expression pattern was variable depending on the samples. Nestin-positive OBLCs were not found in the coronal pulp (Fig. 3a–f). On day 5, the revascularization did not reach the coronal pulp, and the Nestin immunoreaction was limited to the root pulp of the CG (Fig. 3g–i). In contrast, the revascularization was almost completed in the coronal pulp where Nestin-positive newly differentiated OBLCs appeared in the EG (Fig. 3j–l). On day 7, the revascularization was almost completed in the coronal pulp of both the CG and EG (Fig. 3m–q). In the CG, the coronal pulp lacked Nestin-positive OBLCs, although Nestin-positive filamentous structures appeared in the matrix (Fig. 3n, o). In the EG, Nestin-positive OBLCs were observed in the coronal and root pulps, although ankylosis appeared in the pulp floor (Fig. 3p, r). On day 14, Nestin-positive newly differentiated OBLCs were arranged along the pulp-dentin border of the coronal and root pulps of both the CG and EG (Fig. 4a–f). The part of the coronal pulp of the CG lacked Nestin-positive reaction, and the pulp floor suffered from ankylosis in the EG. The coronal and root pulps of the EG contained thick, reparative dentin (Fig. 4d–f). In the CG, Nestin-negative bone-like tissue was induced in the coronal pulp due to the degeneration of

pulp cells including odontoblasts (Fig. 4a–c). The rate of Nestin-positive perimeter of the EG tended to be higher than that of the CG, and the EG showed significant increases in the rate of Nestin-positive perimeter in the distal root compared with the CG on days 5 and 14 (Fig. 4g, h). The amount of the Nestin-positive tertiary dentin in the EG was significantly larger than that in the CG. Whereas the Nestin-negative bone-like tissue increased in amount in the CG compared with that in the EG (Fig. 4i).

3.2 A cell proliferation assay

The timing of active cell proliferation in the EG tended to be sooner than that in the CG, and the peak of cell proliferation in the EG tended to be higher than that in the CG, according to Ki-67 immunostaining in the coronal and root pulps. In the EG, the rate of Ki-67 positive cells of the mesial coronal and root pulps showed peak on day 3 and progressively decreased according to the progress of pulpal healing. In contrast, cell proliferation of the mesial coronal and root pulps reached its peak on day 5 or 7 in the CG (Fig. 5a, c). A significant difference was observed between the EG and CG on day 3 in the mesial root pulp (Fig. 5c). In the EG, the rate of Ki-67 positive cells of the distal coronal and root pulps showed a peak on day 5 and progressively decreased according to the progress of pulpal healing (Fig. 5b, d). Significant differences between EG and

CG were observed on day 5, in the distal coronal and root pulps (Fig. 5b, d).

3.3 TUNEL assay

In the coronal and root pulps on days 3 and 5, the rate of TUNEL-positive cells in the EG tended to be lower than that in the CG. In both groups, the rate of TUNEL-positive cells tended to decrease progressively after its peak on days 3 or 5. In the mesial coronal pulp on day 3 and the distal root pulp on day 5, the rate of TUNEL-positive cells in the EG was substantially lower than in the CG (Fig. 5e–h).

3.4 Morphological changes in long-term cases

In the EG, thick tertiary dentin was observed throughout the pulp cavity where Nestin-positive newly differentiated OBLCs were arranged along the pulp-dentin border except for the perforation site on week four (Fig. 6d, e). In contrast, in the CG, bone-like tissue lacking Nestin immunoreaction occurred in the coronal pulp, and Nestin-positive newly differentiated OBLCs were recognizable in the root pulp and part of the coronal pulp (Fig. 6a, b). The pulp floor of the EG suffered from ankylosis in week four (Fig. 6d, f). In week eight, Nestin-positive tertiary dentin formation was observed in the coronal and root pulps except for the perforation site in the EG. Although ankylosis was not found in

this sample, bone-like tissue development blocked the pulp chamber around the puncture site in the EG (Fig. 6j–l). In contrast, the coronal pulp was replaced by bone-like tissue and occluded, and part of the root was absorbed in the CG (Fig. 6g–i). The number of ERM in the EG tended to be lower than that in the CG, and that in the EG was significantly lower than that in the CG on day 7 (Fig. 6m).

4. Discussion

4.1. Intentional perforation elicits the early revascularization and the activation of dental pulp stem and progenitor cells

This study demonstrated that intentionally perforating the floor of the pulp chamber accelerated the early revascularization after tooth replantation and promoted the differentiation of Nestin-positive OBLCs to form tertiary dentin. The extent of their damage depends on the time that it takes for the establishment of revascularization in the pulp cavity, and the intentionally prolonged time for the completion of tooth replantation worsens the survival of odontoblast-lineage cells [30]. Thus, this study adopted immediate tooth replantation. DPSCs in the perivascular niche of the central pulp and SCAP provide the cell sources that are competent for proliferating during the pulpal healing process after tooth replantation [17]. The progenitor cells of OBLCs

reside in the SOBL [31]. As the damage to pulp cells, including odontoblasts, is limited in the case of tooth drilling, the SOBL cells survive to quickly differentiate into OBLCs without proliferation [29, 32]. In contrast, the SOBL cells are extensively damaged in our study. In addition to odontoblasts in the case of tooth replantation, the cell sources competent for pulpal healing after injury depend on stem and progenitor cells around the perivascular niche of central pulp tissue [19] and SCAP [26], since the SOBL cells are extensively damaged in the case of tooth replantation. The hypoxia activates DPSCs, and active cell proliferation synchronizes with the restoration of blood circulation, and the delayed revascularization leads to the death of DPSCs [25]. On days 5 and 14, the rate of Nestin-positive perimeter in the distal pulp in the EG was substantially higher than in the CG. On day 7, filamentous structures in the CG showed Nestin-positive reaction in the coronal pulp, which is considered a biological response associated with the activation of stem cells [33]. The EG had an earlier peak of active cell proliferation than the CG, and the EG had a greater peak of the cell proliferation than the CG. Furthermore, the rate of TUNEL-positive cells in the EG was lower than that in the CG on days 3 and 5, indicating that apoptosis in the pulp cavity after tooth replantation was suppressed in the EG. These results suggest that early establishment of revascularization via the perforation in the EG reduced the number of apoptotic cells in

the pulp chamber and that more progenitor and stem cells survived in the perivascular niche of central pulp tissue than those in the CG to actively proliferate thereafter.

In the EG, the arrangement of Nestin-positive OBLCs along the pulp-dentin border to form tertiary dentin formation was observed on day 14 after operation. A previous study demonstrated that the maintenance of pulp quiescent stem/progenitor cells is a decisive factor in inducing OBLC differentiation [7]. Thus, pulp quiescent stem/progenitor cells were maintained after tooth replantation in the EG. In addition, in the CG, the amount of tertiary dentin was significantly smaller and the bone-like tissue formation was significantly larger compared with those in the EG. In the CG, delayed revascularization, particularly in the coronal pulp far from the apical foramina, hampered pulpal healing, resulting in a stagnation of the inflammatory response and, as a result, the death of pulp stem and progenitor cells capable of differentiating into OBLCs, inhibiting tertiary dentin formation and inducing bone-like tissue formation. The amount of bone-like tissue was significantly larger in the CG, suggesting that the different dynamics of pulp stem and progenitor cells may occur in the EG and CG. In the CG, the pulp stem and progenitor cells in the perivascular niche of central pulp tissue are extensively degenerated, and the pulpal healing depends on SCAP at the apical foramina for the cell sources for OBLCs, resulting in the delayed arrival of pulp

stem and progenitor cells to the coronal pulp. The delayed arrival of stem and progenitor cells to the coronal pulp may be a decisive factor for the formation of bone-like tissue. Because the absence of odontoblast-lineage cells including dental pulp stem and progenitor cells for a long time elicits the osteoblast differentiation in the CG group [7], the delayed arrival of SCAP into the coronal pulp may provide the circumstance suitable for bone-like tissue formation compared with the EG group with the presence of DPSCs in the perivascular niche of the central pulp. However, whether bone-like tissue-forming cells are derived from the inherent or no-inherent pulp cells (for example, bone marrow-derived cells) remains to be clarified. In the experimental model for tooth replantation using two-week-old mice with short roots and three-week-old mice with long roots, the patterns of pulpal healing differ dramatically in these two animals [33], suggesting that the distance between the injury site and the stem cell niche dramatically impacts the pulpal healing.

4.2. The considerable issues in the current experimental model: induction of ankylosis and impact on epithelial cell rests of Malassez

The EG suffered ankylosis after postoperative day 7. The number of ERM tended to be lower with a significant decrease on day 7 in the EG compared with that in the CG.

Experimentally reducing the ERM has been reported to induce ankylosis [28], suggesting that they may be involved in the maintenance of periodontal space. In this study, the induction of ankylosis in the EG may be attributed to a decrease in the number of ERM caused by perforation at the pulp chamber floor. Even in the EG, however, several samples did not suffer from ankylosis at the pulp floor, suggesting that ankylosis may be avoided by minimizing the damage to the periodontal tissue, e.g., the reduction in the size of the perforation. Due to the technical limitation in reducing the size of perforation in the experiment using mice, further experiments using larger animals such as rats with smaller sizes of perforation relative to the tooth size are needed to explore conditions to prevent ankylosis.

4.3. The benefit of perforation at the pulp chamber's floor and its clinical significance

Compared with the experimental root resection [25], the pulp floor perforation promotes pulpal healing by maintaining the SCAP at the root apexes. Generally, endodontic treatment is necessary after replantation of avulsed teeth with mature roots since the survival of the pulp tissue is not expected [1]. This technique may induce revascularization in the pulp cavity via perforation, even in teeth with mature roots, and provides a putative new treatment method with regeneration of the pulp tissue in

avulsed teeth with mature roots. This strategy could be applied to the autotransplantation procedure of multirooted teeth, such as the transplantation of third molars to the other area, since perforating at the floor of the pulp chamber may contribute to success in the transplantation without pulp extraction during and after treatment. It is not easy to apply the concept of pulpal floor perforation to the treatment for avulsed teeth, because the teeth that are usually avulsed are anterior teeth, not multirooted molars. The clinical application of this concept requires the establishment and validation of an experimental model for perforating the lateral side of the root. The finding that accidental root fractures in the mouse model may induce early revascularization at the fracture site supports the usefulness of lateral root perforation.

5. Conclusions

This study demonstrated that intentionally perforating the floor of the pulp chamber provides a route *via* the floor for early revascularization, resulting in the better pulpal healing after tooth replantation. This new method could be expected to preserve the root length and presence of the SCAPs and contribute to improving the pulpal healing of avulsed teeth. The clinical application of this concept to the treatment of avulsed teeth requires the establishment and validation of an experimental model for perforating the

lateral side of the root.

References

[1] Fouad AF, Abbott PV, Tsilingaridis G, Cohenca N, Lauridsen E, Bourguignon C, O'Connell A, Flores MT, Day PF, Hicks L, Andreasen JO, Cehreli ZC, Harlamb S, Kahler B, Oginni A, Semper M, Levin L. International Association of Dental Traumatology guidelines for the management of traumatic dental injuries: 2. Avulsion of permanent teeth. Dental traumatol. 2020;36:331-42.

[2] Andreasen JO, Borum MK, Jacobsen HL, Andreasen FM. Replantation of 400 avulsed permanent incisors. 1. Diagnosis of healing complications. Endod Dent Traumatol. 1995;11:51-8.

[3] Souza BDM, Dutra KL, Kuntze MM, Bortoluzzi EA, Flores-Mir C, Reyes-Carmona J, Felippe WT, Porporatti AL, De Luca Canto G. Incidence of root resorption after the replantation of avulsed teeth: A meta-analysis. J Endod. 2018;44:1216-27.

[4] Meng M, Chen Y, Ren H, Zhang Q, Chen S, Zhou X, Zou J. Effect of tetracyclines on pulpal and periodontal healing after tooth replantation: a systematic review of human and animal studies. Bmc Oral Health.

2021;21:289.

[5] Tsukamoto-Tanaka H, Ikegame M, Takagi R, Harada H, Ohshima H. Histochemical and immunocytochemical study of hard tissue formation in dental pulp during the healing process in rat molars after tooth replantation. Cell Tissue Res. 2006;325:219-29.

[6] Mutoh N, Nakatomi M, Ida-Yonemochi H, Nakagawa E, Tani-Ishii N, Ohshima H. Responses of BrdU label-retaining dental pulp cells to allogenic tooth transplantation into mouse maxilla. Histochem Cell Biol. 2011;136:649-61.

[7] Saito K, Ohshima H. Differentiation capacity and maintenance of dental pulp stem/progenitor cells in the process of pulpal healing following tooth injuries. J Oral Biosci. 2017;59:63-70.

[8] Lenstrup K, Skleller V. A follow-up study of teeth replanted after accidental loss. Acta Odontol Scand. 1959;17:503-9.

[9] Ohman A. Healing and sensitivity to pain in young replanted human teeth. An experimental, clinical and histological study. Odontol Tidskr. 1965;73:165-228.

[10] Andreasen JO, Hjorting-Hansen E. Replantation of teeth. I. Radiographic and clinical study of 110 human teeth replanted after accidental loss. Acta Odontol Scand. 1966;24:263-86.

[11] Skoglund A, Tronstad L. Pulpal changes in replanted and autotransplanted immature teeth of dogs. J Endod. 1981;7:309-16.

[12] Skoglund A. Pulpal changes in replanted and autotransplanted apicoectomized mature teeth of dogs. Int J Oral Surgy. 1981;10:111-21.

[13] Andreasen FM. Pulpal healing after luxation injuries and root fracture in the permanent dentition. Endod Dent Traumatol. 1989;5:111-31.

[14] Li L, Clevers H. Coexistence of quiescent and active adult stem cells in mammals. Science. 2010;327:542-5.

[15] Ishikawa Y, Ida-Yonemochi H, Nakakura-Ohshima K, Ohshima H. The relationship between cell proliferation and differentiation and mapping of putative dental pulp stem/progenitor cells during mouse molar development by chasing BrdU-labeling. Cell Tissue Res. 2012;348:95-107.

[16] Ishikawa Y, Ida-Yonemochi H, Saito K, Nakatomi M, Ohshima H. The Sonic hedgehog–Patched–Gli signaling pathway maintains dental epithelial and pulp stem/progenitor cells and regulates the function of odontoblasts. Front Dent Med. 2021;2:651334.

[17] Ishikawa Y, Ida-Yonemochi H, Suzuki H, Nakakura-Ohshima K, Jung HS, Honda MJ, Ishii Y, Watanabe N, Ohshima H. Mapping of BrdU label-retaining

dental pulp cells in growing teeth and their regenerative capacity after injuries. Histochem Cell Biol. 2010;134:227-41.

[18] Aizawa C, Saito K, Ohshima H. Regulation of IGF-I by IGFBP3 and IGFBP5 during odontoblast differentiation in mice. J Oral Biosci. 2019;61:157-62.

[19] Saito K, Ohshima H. The putative role of insulin-like growth factor (IGF)-binding protein 5 independent of IGF in the maintenance of pulpal homeostasis in mice. Regen Ther. 2019;11:217-24.

[20] Saito K, Nakatomi M, Kenmotsu S, Ohshima H. Allogenic tooth transplantation inhibits the maintenance of dental pulp stem/progenitor cells in mice. Cell Tissue Res. 2014;356:357-67.

[21] Saito K, Nakatomi M, Ohshima H. Dynamics of bromodeoxyuridine label-retaining dental pulp cells during pulpal healing after cavity preparation in mice. J Endod. 2013;39:1250-5.

[22] Nakaki T, Nakakura-Ohshima K, Nakagawa E, Ishikawa Y, Saito K, Ida-Yonemochi H, Ohshima H. Donor–host tissue interaction in allogenic transplanted tooth germ with special reference to periodontal tissue. J Oral Biosci. 2018;60:21-30.

[23] Nakaki T, Saito K, Ida-Yonemochi H, Nakagawa E, Kenmotsu S, Ohshima H.

Contribution of donor and host mesenchyme to the transplanted tooth germs. J Dent Res. 2015;94:112-20.

[24] Ida-Yonemochi H, Nakatomi M, Ohshima H. Establishment of in vitro culture system for evaluating dentin-pulp complex regeneration with special reference to the differentiation capacity of BrdU label-retaining dental pulp cells. Histochem Cell Biol. 2014;142:323-33.

[25] Nakakura-Ohshima K, Quispe-Salcedo A, Sano H, Hayasaki H, Ohshima H. The effects of reducing the root length by apicoectomy on dental pulp revascularization following tooth replantation in mice. Dental traumatol. 2021;37:677-90.

[26] Sonoyama W, Liu Y, Fang D, Yamaza T, Seo BM, Zhang C, Liu H, Gronthos S, Wang CY, Shi S, Wang S. Mesenchymal stem cell-mediated functional tooth regeneration in swine. PLoS One. 2006;1:e79.

[27] Bakopoulou A, Leyhausen G, Volk J, Tsiftsoglou A, Garefis P, Koidis P, Geurtsen W. Comparative analysis of in vitro osteo/odontogenic differentiation potential of human dental pulp stem cells (DPSCs) and stem cells from the apical papilla (SCAP). Arch Oral Biol. 2011;56:709-21.

[28] Fujiyama K, Yamashiro T, Fukunaga T, Balam TA, Zheng L, Takano-

Yamamoto T. Denervation resulting in dento-alveolar ankylosis associated with decreased Malassez epithelium. J Dent Res. 2004;83:625-9.

[29] Imai C, Sano H, Quispe-Salcedo A, Saito K, Nakatomi M, Ida-Yonemochi H, Okano H, Ohshima H. Exploration of the role of the subodontoblastic layer in odontoblast-like cell differentiation after tooth drilling using Nestin-enhanced green fluorescent protein transgenic mice. J Oral Biosci. 2022;64:77-84.

[30] Hasegawa T, Suzuki H, Yoshie H, Ohshima H. Influence of extended operation time and of occlusal force on determination of pulpal healing pattern in replanted mouse molars. Cell Tissue Res. 2007;329:259-72.

[31] Nakatomi M, Quispe-Salcedo A, Sakaguchi M, Ida-Yonemochi H, Okano H, Ohshima H. Nestin expression is differently regulated between odontoblasts and the subodontoblastic layer in mice. Histochem Cell Biol. 2018;149:383-91.

[32] Harada M, Kenmotsu S, Nakasone N, Nakakura-Ohshima K, Ohshima H. Cell dynamics in the pulpal healing process following cavity preparation in rat molars. Histochem Cell Biol. 2008;130:773-83.

[33] Suzuki-Barrera K, Makishi S, Nakatomi M, Saito K, Ida-Yonemochi H, Ohshima H. Role of osteopontin in the process of pulpal healing following tooth replantation in mice. Regen Ther. 2022;21:460-8.

Figure legends

Fig. 1 Number of maxillae in each experiment and for statistical analysis after tooth replantation. IHC, immunohistochemistry.

Fig. 2 Nestin immunohistochemical section of an untreated 4-week-old mouse molar. The b, c, and d are the higher magnified views of the boxed areas in a, b, and b, respectively. (a–d) Differentiated odontoblasts showed Nestin-positive reaction throughout the dental pulp. The coronal odontoblasts show pseudostratified features (c), whereas the cells at the pulp floor exhibit cuboidal shape (d). D, dentin; DP, dental pulp; OB, odontoblasts. Scale bars = (a) 500 μm, (b) 250 μm, (c, d) 50 μm.

Fig. 3 Hematoxylin & eosin (H&E) stained (a, d, g, j, m, p) and Nestin immunohistochemical sections (b, c, e, f, h, i, k, l, n, o, q, r) of the replanted teeth in the control group (CG) (a–c, g–i, m–o) and experimental group (EG) (d–f, j–l, p–r) 3 (a–f), 5 (g–l), and 7 days (m–r) after tooth replantation. The insets in d, j, and p are the higher magnified views of the boxed areas in d, j, and p, respectively. The c, f, i, l, o, and r are the higher magnified views of the boxed areas in b, e, h, k, n, and q, respectively. (a–f)

Nestin expression is observed in the survived odontoblasts or newly differentiated odontoblast-like cells (OBLCs) beneath the root pulp of the CG and EG. The coronal pulp lacks Nestin-positive OBLCs. (g–i) Revascularization does not reach the coronal pulp, and the Nestin immunoreaction is limited in the root pulp. (j–l) Revascularization is almost completed in the coronal pulp where Nestin-positive newly differentiated OBLCs appear. (m–r) Revascularization is almost completed even in the coronal pulp of the CG. The coronal pulp lacks Nestin-positive OBLCs, and Nestin-positive filamentous structures appear in the matrix in the CG. Nestin-positive OBLCs are observed in the coronal and root pulps, although ankylosis appears in the pulp floor in the EG. D, dentin; DP, dental pulp; AB, alveolar bone. Scale bars = (a, b, d, e, g, h, j, k, m, n, p, q) 500 μm, (c, f, i, l, o, r, insets) 100 μm.

Fig. 4 H&E stained (a, d) and Nestin immunohistochemical sections (b, c, e, f) of the replanted teeth in the CG (a–c) and EG (d–f) 14 days after tooth replantation (a–f) and the rates of Nestin-positive perimeter in the mesial (g) and distal pulps (h) during days 3–14 and Nestin-positive/negative hard tissue formation in the pulp cavity on day 14 (i). The insets in a and d are the higher magnified views of the boxed areas in a and d, respectively. The c and f are the higher magnified views of the boxed areas in b and e,

respectively. (a–f) Nestin-positive newly differentiated OBLCs arrange along the pulp-dentin border of the coronal and root pulps of both the CG and EG except for the part of coronal pulp of the CG and the pulp floor suffered from ankylosis in the EG. Nestin-negative bone-like tissue is induced in the coronal pulp in the CG. The coronal and root pulps of the EG contain thick reparative dentin. (g, h) The rate of Nestin-positive perimeter of the EG tends to be higher than that of the CG, and the EG shows significant increases in the rate of Nestin-positive perimeter in the distal root compared with the CG on days 5 and 14. (i) The amount of the Nestin-positive tertiary dentin in the EG is significantly larger than that in the CG, whereas the Nestin-negative bone-like tissue increases in amount in the CG compared with that in the EG. D, dentin; DP, dental pulp; AB, alveolar bone, TD; tertiary dentin, B; bone-like tissue. Scale bars = (a, b, d, e) 500 μm, (c, insets) 100 μm, (f) 50 μm.

Fig. 5 The rates of Ki-67- (a–d) and TUNEL-positive cells (e–h) in the mesial (a, c, e, g) and distal (b, d, f, h) coronal (a, b, e, f) and root pulps (c, d, g, h) during days 3–14. (a–d) The timing of active cell proliferation in the EG tends to occur earlier than that in the CG, and the peak of the cell proliferation in the EG tends to be higher than that in the CG. The rate of positive cells of the mesial coronal and root pulps shows the peak

on day 3 and progressively decreases according to the progress of pulpal healing in the EG. Cell proliferation of the mesial coronal and root pulps reaches the peak on day 5 or 7 in the CG. A significant difference is observed between the EG and CG on day 3 in the mesial root pulp. The rate of positive cells of the distal coronal and root pulps shows the peak on day 5 and progressively decreases according to the progress of pulpal healing in the EG. Significant differences between EG and CG are observed on day 5 in the distal coronal and root pulps. (e–h) In the coronal and root pulps on days 3 and 5, the rate of positive cells in the EG tends to be lower than that in the CG. the rate of TUNEL-positive cells tends to decrease progressively after its peak on days 3 or 5 in both groups. The rate of positive cells in the EG is significantly lower than that in the CG in the mesial coronal pulp on day 3 and the distal root pulp on day 5.

Fig. 6 H&E stained (a, d, g, j) and Nestin immunohistochemical sections (b, e, h, k) and μCT images (c, f, i, l) of the replanted teeth in the CG (a–c, g–i) and EG (d–f, j–l) 4 (a–f) and 8 weeks (g–l) after tooth replantation and the number of ERM per unit area of the periodontal ligament during days 3–14 (m). (a–c) Bone-like tissue lacking Nestin immunoreaction occurs in the coronal pulp, and Nestin-positive newly differentiated OBLCs are recognizable in the root pulp and part of the coronal pulp. (d–f) Thick

tertiary dentin is observed throughout the pulp cavity where Nestin-positive newly differentiated OBLCs arrange along the pulp-dentin border except for the perforation site with ankylosis. (g–i) The coronal pulp is replaced by bone-like tissue and occludes, and part of the root is absorbed. (j–l) Nestin-positive tertiary dentin formation is observed in the coronal and root pulps. The ankylosis is not observed in this sample. (m) The number of ERM in the EG tends to be lower than that in the CG, and that in the EG is significantly lower than that in the CG on day 7. D, dentin; DP, dental pulp; AB, alveolar bone, TD; tertiary dentin, B; bone-like tissue. Scale bars = (a–l) 500 μm, (insets) 50 μm.

Fig. 1

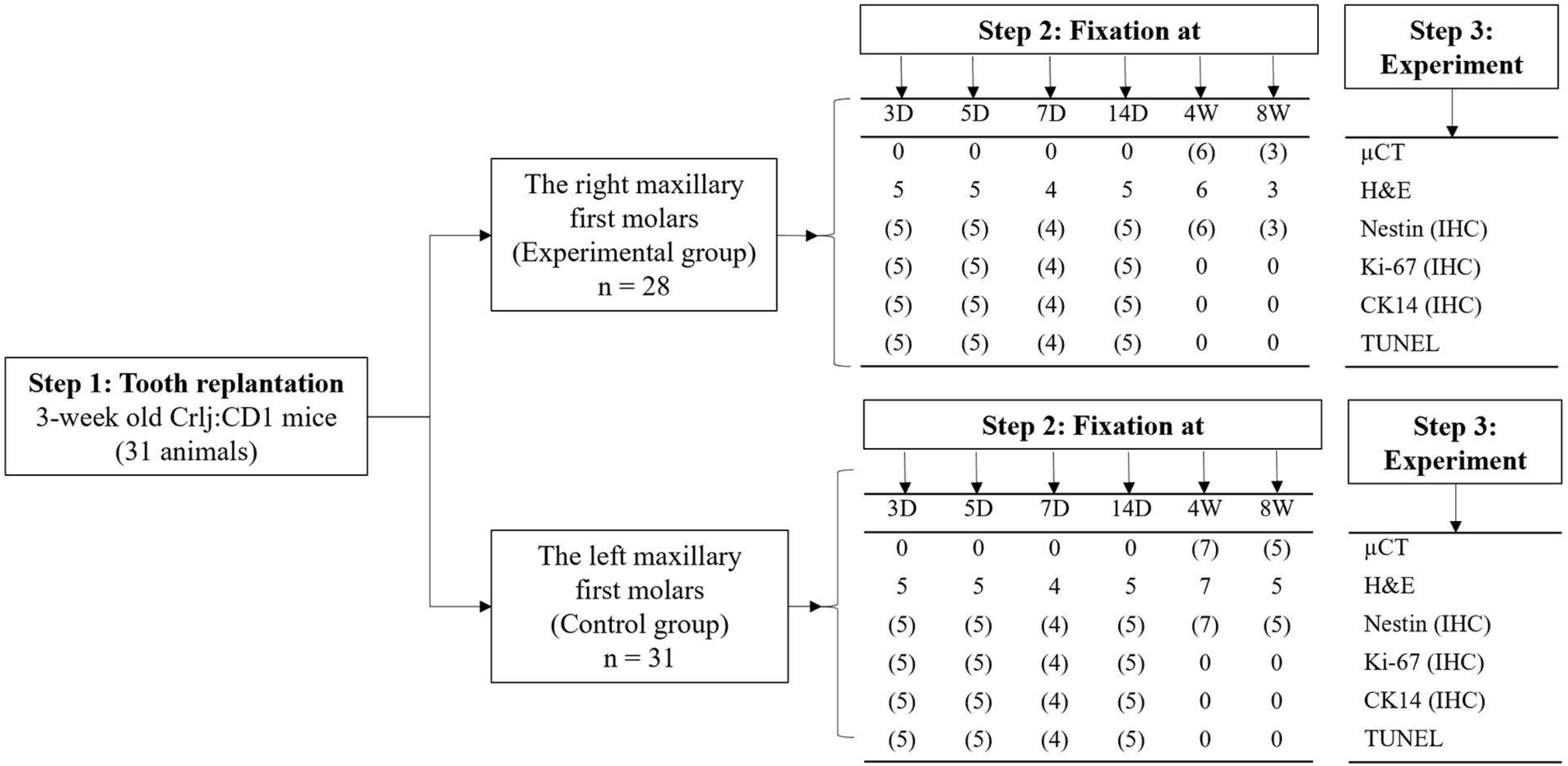
Step 1: Tooth replantation
3-week old Crlj:CD1 mice
(31 animals)
The right maxillary first molars (Experimental group) n = 28
The left maxillary first molars (Control group) n = 31
Step 2: Fixation at
3D 5D 7D 14D 4W 8W
0 0 0 0 (6) (3)
5 5 4 5 6 3
(5) (5) (4) (5) (6) (3)
(5) (5) (4) (5) 0 0
(5) (5) (4) (5) 0 0
(5) (5) (4) (5) 0 0
Step 3: Experiment
μCT
H&E
Nestin (IHC)
Ki-67 (IHC)
CK14 (IHC)
TUNEL
Step 2: Fixation at
3D 5D 7D 14D 4W 8W
0 0 0 0 (7) (5)
5 5 4 5 7 5
(5) (5) (4) (5) (7) (5)
(5) (5) (4) (5) 0 0
(5) (5) (4) (5) 0 0
(5) (5) (4) (5) 0 0
Step 3: Experiment
μCT
H&E
Nestin (IHC)
Ki-67 (IHC)
CK14 (IHC)
TUNEL

Fig. 2

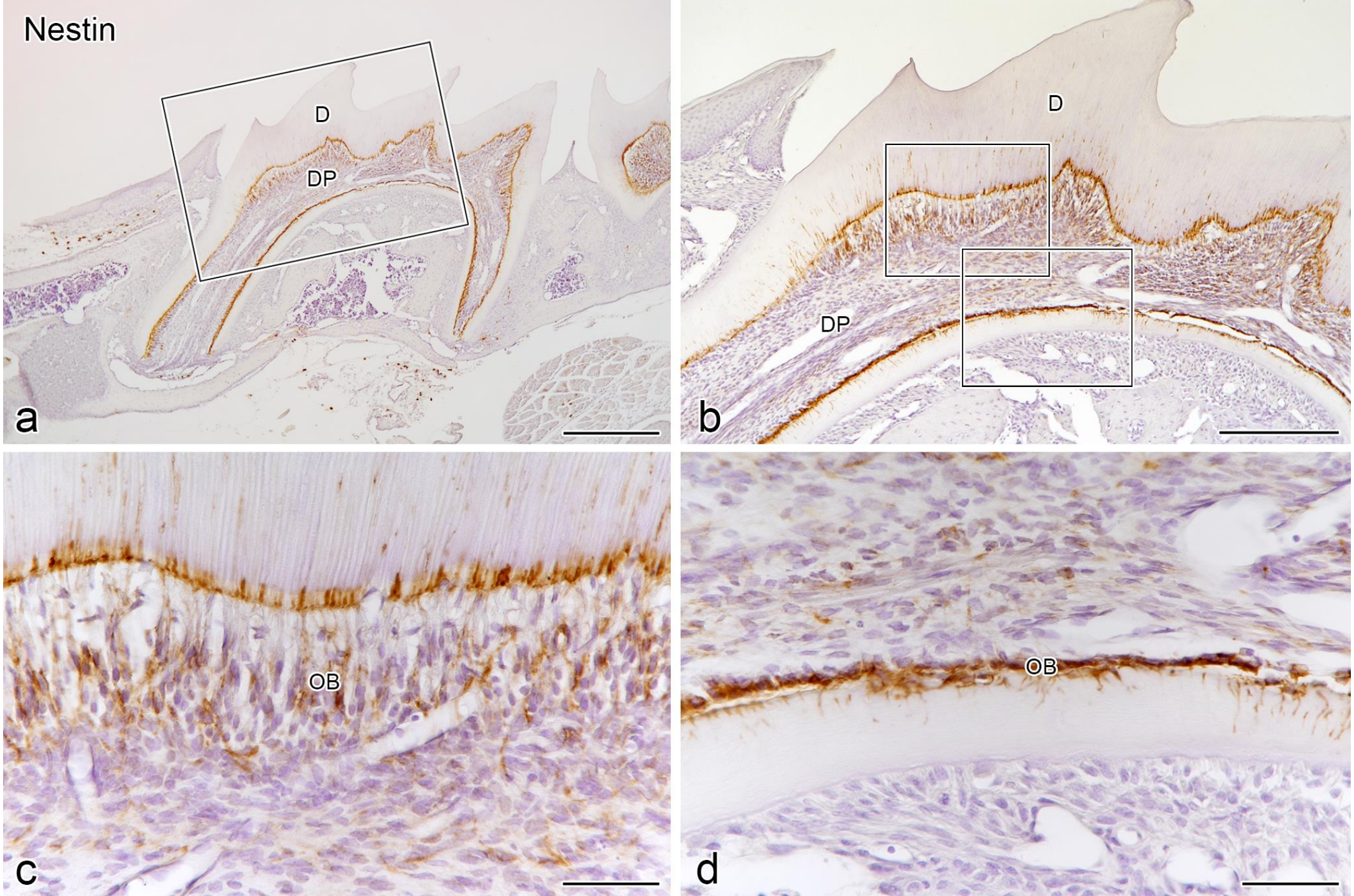

Fig. 3

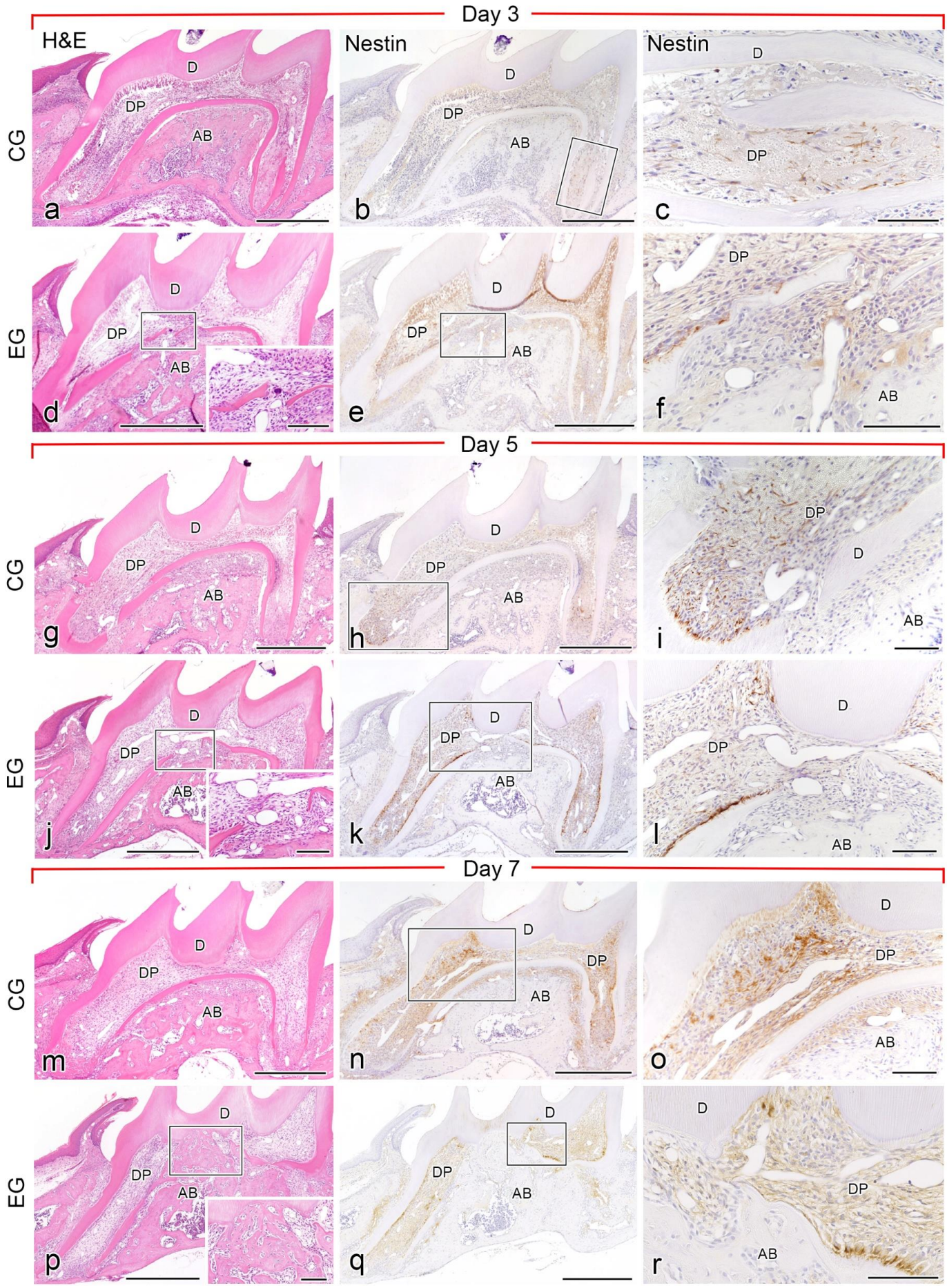
Day 3
Day 5
Day 7
CG
EG
H&E
Nestin
Nestin
D
DP
AB
a
b
c
d
e
f
g
h
i
j
k
l
m
n
o
p
q
r

Fig. 4

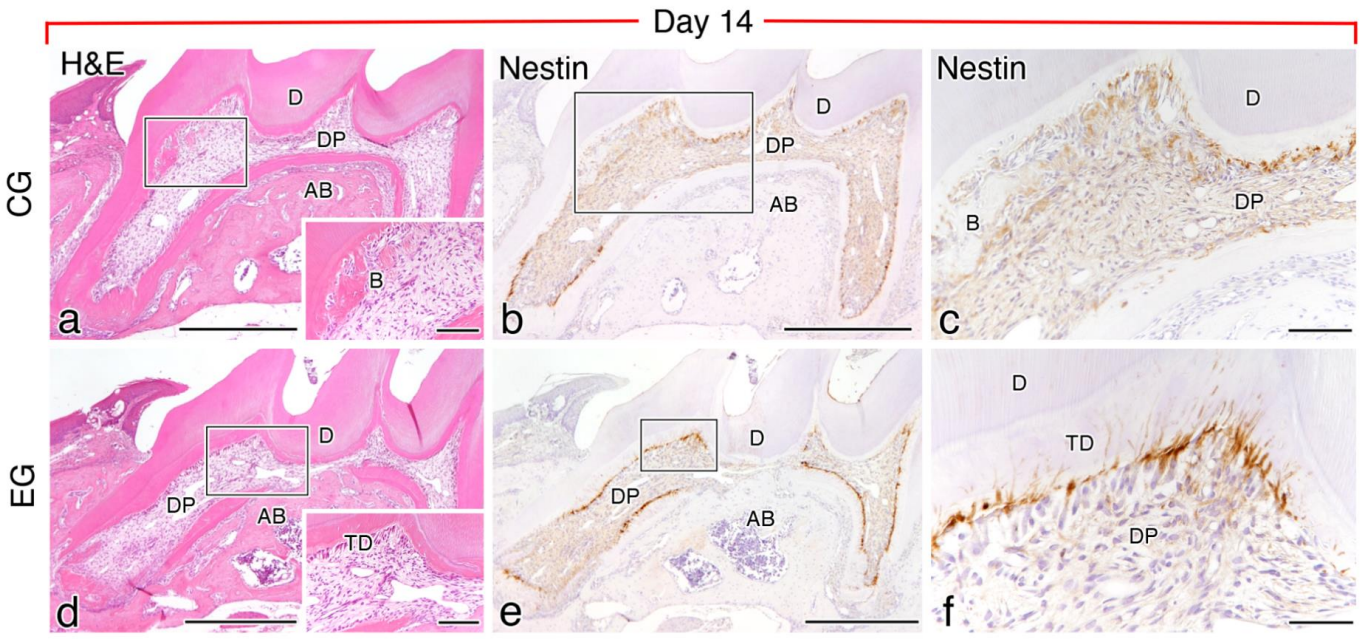
Day 14
H&E
Nestin
Nestin
CG
EG
D
DP
AB
B
TD
a
b
c
d
e
f

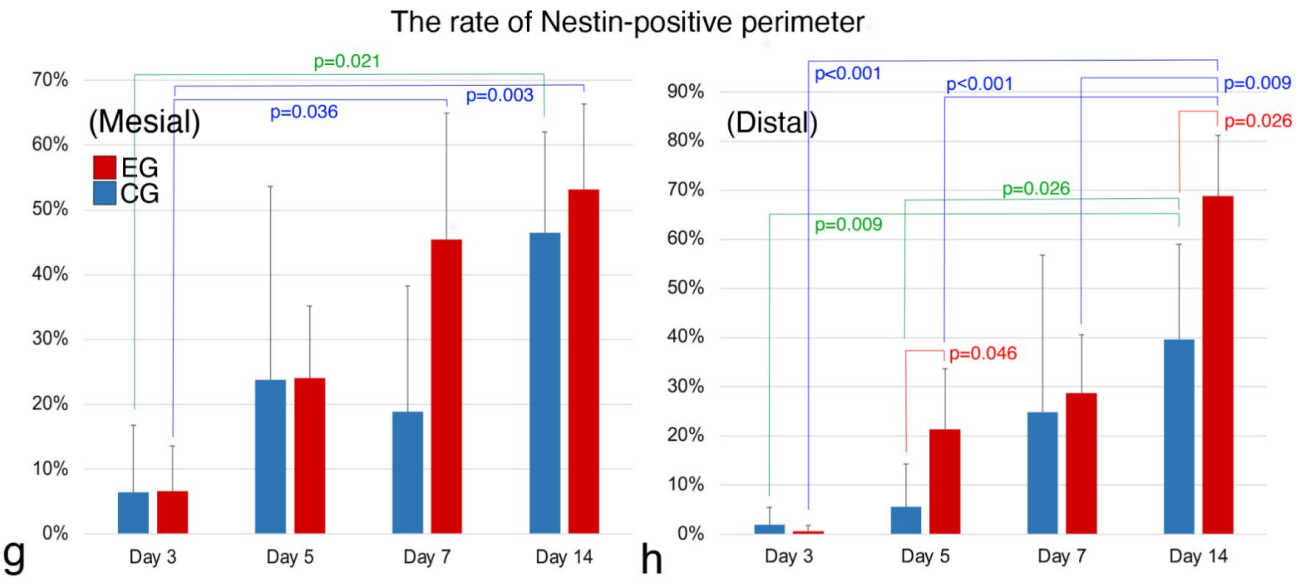
The rate of Nestin-positive perimeter
(Mesial)
EG
CG
p=0.021
p=0.036
p=0.003
70%
60%
50%
40%
30%
20%
10%
0%
Day 3
Day 5
Day 7
Day 14
g
(Distal)
p<0.001
p<0.001
p=0.009
p=0.026
p=0.009
p=0.026
p=0.046
90%
80%
70%
60%
50%
40%
30%
20%
10%
0%
Day 3
Day 5
Day 7
Day 14
h

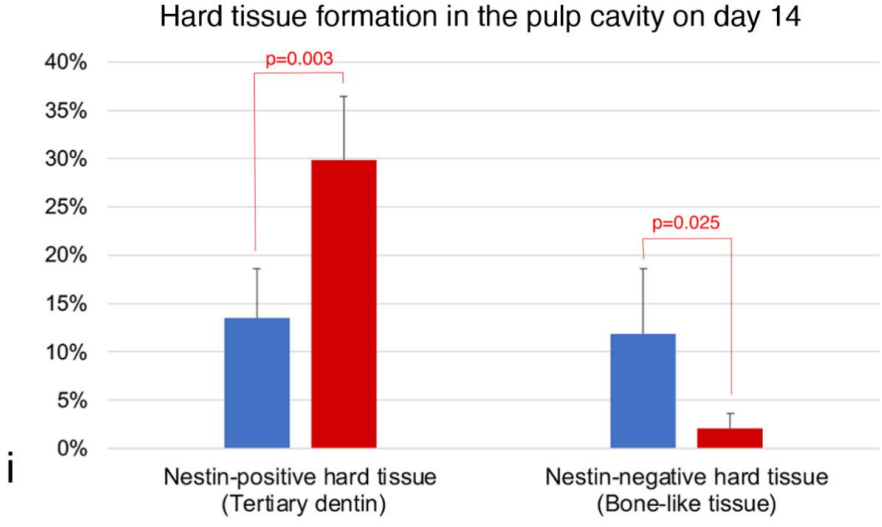
Hard tissue formation in the pulp cavity on day 14
p=0.003
p=0.025
40%
35%
30%
25%
20%
15%
10%
5%
0%
Nestin-positive hard tissue
(Tertiary dentin)
Nestin-negative hard tissue
(Bone-like tissue)
i

Fig. 5

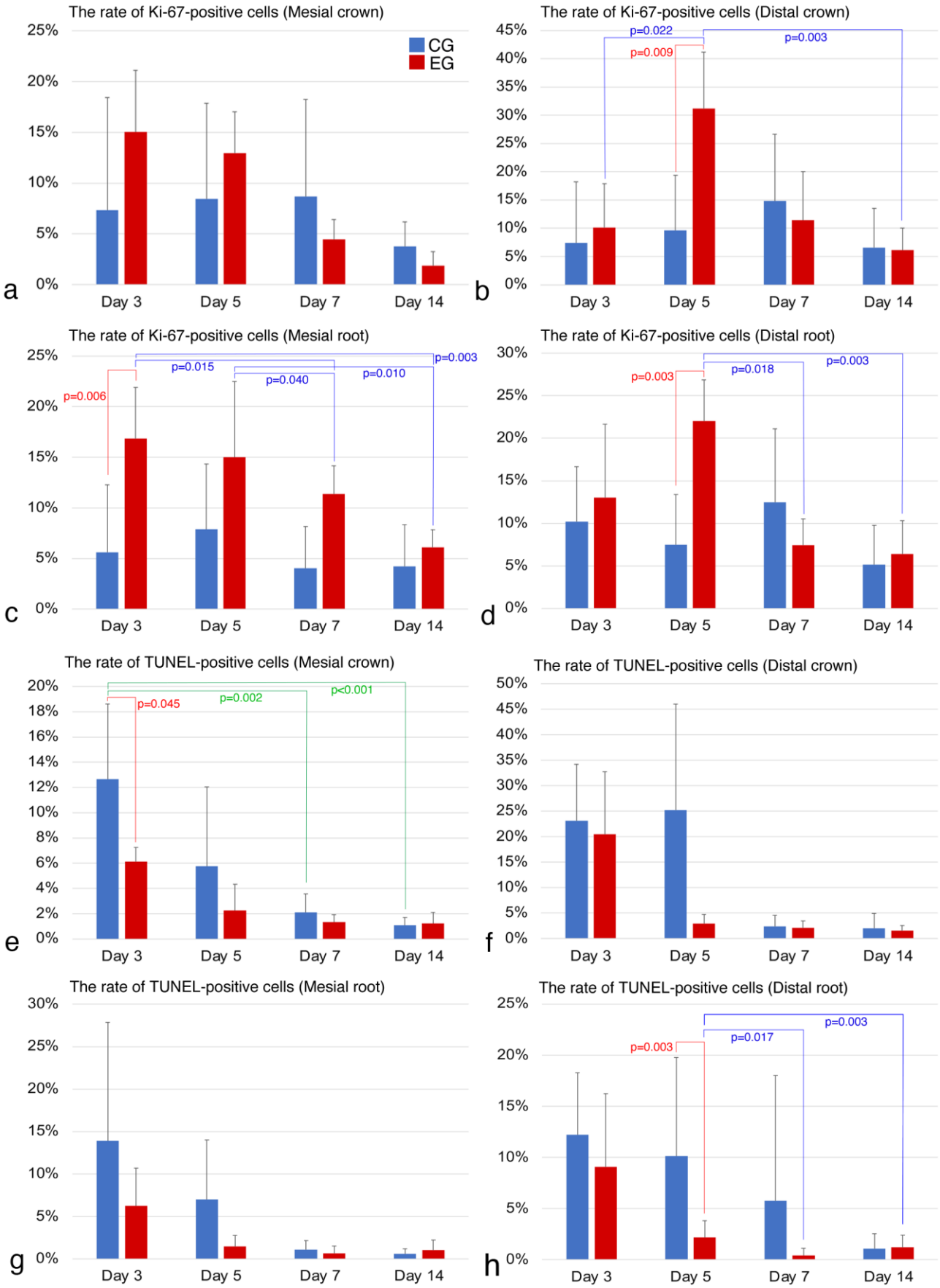
a
The rate of Ki-67-positive cells (Mesial crown)
CG
EG
25%
20%
15%
10%
5%
0%
Day 3
Day 5
Day 7
Day 14
b
The rate of Ki-67-positive cells (Distal crown)
p=0.022
p=0.009
p=0.003
45%
40%
35%
30%
25%
20%
15%
10%
5%
0%
Day 3
Day 5
Day 7
Day 14
c
The rate of Ki-67-positive cells (Mesial root)
p=0.006
p=0.015
p=0.040
p=0.010
p=0.003
25%
20%
15%
10%
5%
0%
Day 3
Day 5
Day 7
Day 14
d
The rate of Ki-67-positive cells (Distal root)
p=0.003
p=0.018
p=0.003
30%
25%
20%
15%
10%
5%
0%
Day 3
Day 5
Day 7
Day 14
e
The rate of TUNEL-positive cells (Mesial crown)
p=0.045
p=0.002
p<0.001
20%
18%
16%
14%
12%
10%
8%
6%
4%
2%
0%
Day 3
Day 5
Day 7
Day 14
f
The rate of TUNEL-positive cells (Distal crown)
50%
45%
40%
35%
30%
25%
20%
15%
10%
5%
0%
Day 3
Day 5
Day 7
Day 14
g
The rate of TUNEL-positive cells (Mesial root)
30%
25%
20%
15%
10%
5%
0%
Day 3
Day 5
Day 7
Day 14
h
The rate of TUNEL-positive cells (Distal root)
p=0.003
p=0.017
p=0.003
25%
20%
15%
10%
5%
0%
Day 3
Day 5
Day 7
Day 14

Fig. 6

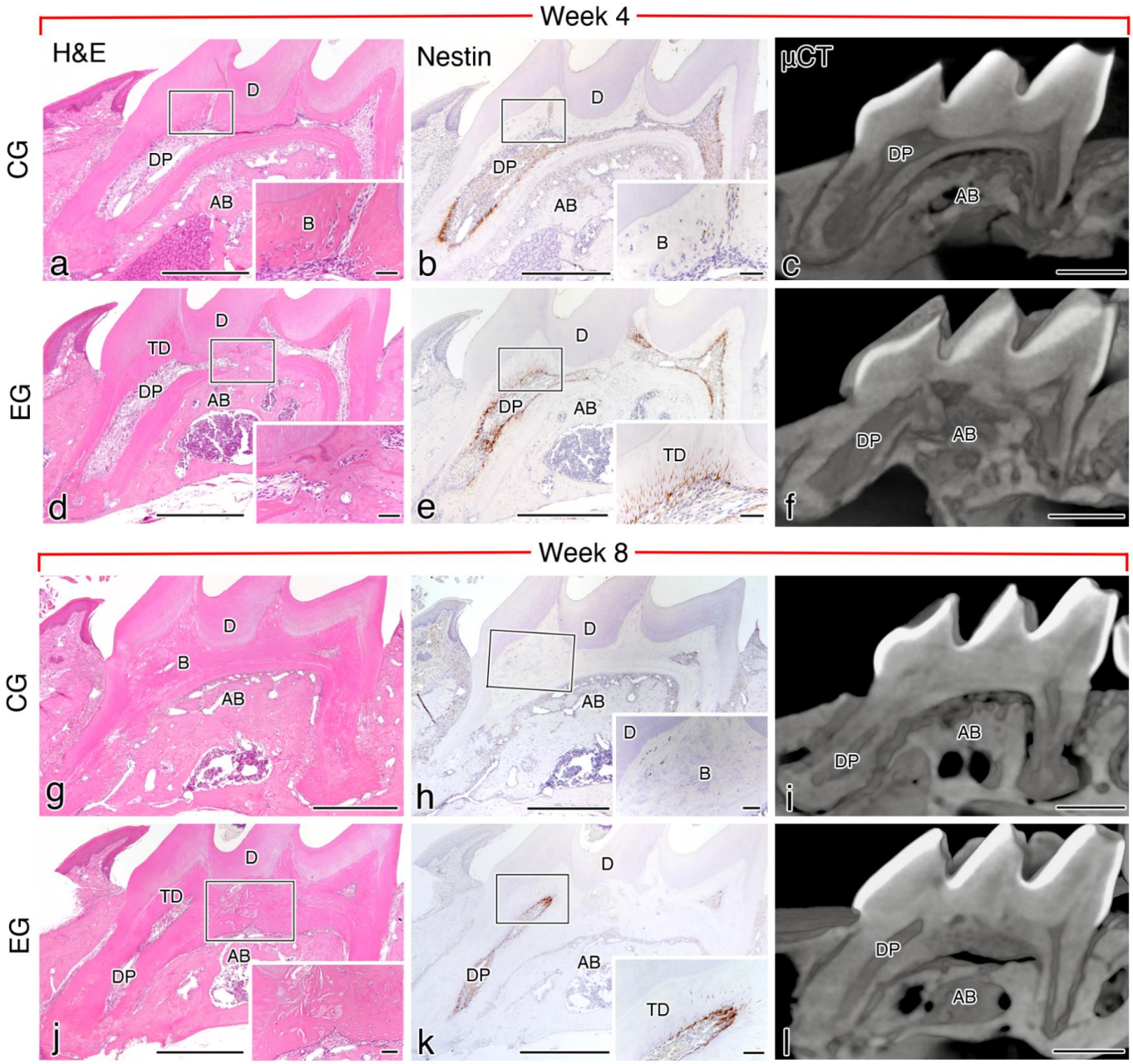
Week 4
H&E
Nestin
μCT
CG
EG
D
DP
AB
B
TD
a
b
c
d
e
f
Week 8
g
h
i
j
k
l

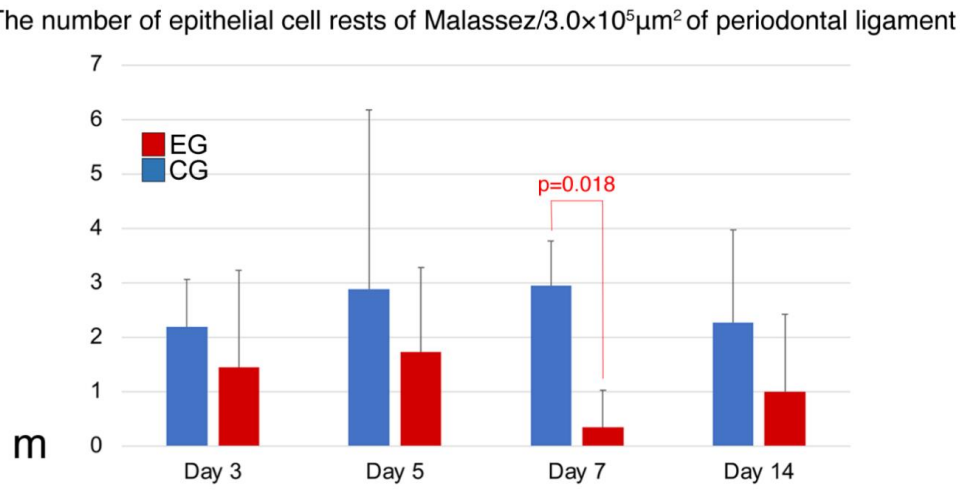
The number of epithelial cell rests of Malassez/3.0×10⁵μm² of periodontal ligament
m
EG
CG
p=0.018
0
1
2
3
4
5
6
7
Day 3
Day 5
Day 7
Day 14